ELSEVIER

Nuclear Instruments and Methods in Physics Research A 461 (2001) 440–448

NUCLEAR INSTRUMENTS & METHODS IN PHYSICS RESEARCH Section A

www.elsevier.nl/locate/nima

The analog signal processor of the Auger fluorescence detector prototype

S. Argirò[a], D.V. Camin[a,*], P. Cattaneo[b], M. Destro[a], R. Fonte[c,1], R. Gariboldi[a], V. Grassi[a], M. Lapolla[a], P.F. Manfredi[b], E. Menichetti[d], M. Nicotra[c], P. Privitera[e], L. Ratti[b], V. Re[f], V. Speziali[b], P. Trapani[d]

[a] *Dipartimento de fisica, Università degli studi di Milano and INFN, Via Celoria 16, 1-20133 Milano, Italy*
[b] *Università di Pavia and INFN, Italy*
[c] *INFN, Sezione di Catania, Italy*
[d] *Università di Torino and INFN, Italy*
[e] *Università di Roma II, and INFN, Italy*
[f] *Università di Bergamo and INFN, Italy*

Abstract

The Auger Fluorescence Detector will allow to determine the longitudinal development of atmospheric showers in the range 10^{19}–10^{21} eV. A detector module comprises an array of 20×22 PMTs at the focal surface of a large-aperture telescope. Thirty such modules will be used. The PMTs pixel signal is variable in shape depending on the shower-eye geometry. The sky background light (BL) is also variable. We have developed an analog signal processor to obtain best energy and timing resolution despite those constrains. The Head Electronics (HE) bias the PMTs and keeps its pulse-gain constant even for large BL. This is measured using a current-monitor of novel design. Both the signal pulse and the BL DC level are sent via a single twisted pair to the Analog Board (AB). The AB performs the compression of the 15–16 bit signal dynamic range into 12 bits of the FADC which follows the AB. A three-pole Bessel filter was adopted for antialiasing. The AB includes 16 bit sigma-delta chips to readout the BL DC level, and a test-pulse distribution system.

PACS: 29.40

Keywords: Analog signal processing; Ultra-high-energy cosmic rays; Photomultipliers

1. Introduction

The Pierre Auger Project aims at increasing substantially the so far scarce statistics of ultra-high-energy cosmic rays (UHECR) above the Greisen–Zatsepin–Kuzmin (GZK) cutoff, i.e. from $\sim 10^{19}$ to 10^{21} eV. In the last 30 years, a few events above 10^{20} eV have been detected by previous experiments [1–4]. The location of their sources should be extragalactic although not very far ($\sim$ 50 Mpc) in cosmological terms. The mere existence of those events is puzzling as there are no known mechanisms capable to generate or accelerate light particles to such enormous energies.

*Corresponding author.
E-mail address: camin@mi.infn.it (D.V. Camin).
[1] Also at University of Albuquerque, New Mexico, USA

0168-9002/01/$ - see front matter
PII: S0168-9002(00)01269-9

The Auger Project comprises two observatories in both Hemispheres each one covering an area of 3000 km^2 in a flat and desert land at above 1500 mt above sea level. An array of 1600 water Cherenkov detectors with an area of 10 m^2, separated by 1.5 km will be sensible to the shower front as it reaches the ground level. Each tank of the Surface Detector array (SD) comprises a set of three PMTs and related amplification and trigger electronics, a GPS system used for timing synchronization, a communication system similar to that used in cellular phones and a solar panel which provides the necessary electrical power. In addition, a Fluorescence Detector (FD) will allow to record the longitudinal development of the shower as it progress from the higher atmosphere up to the ground level. This detector will operate during dark nights and will allow to see at least the 10% of the events in coincidence with the SD, allowing cross calibration of both detectors, and therefore reducing the systematics errors. The use of hybrid techniques by the Auger experiment is a powerful tool that has so far not been used in other UHECR experiments [5]. The number of events with energies of $\sim 10^{20}$ eV will be about 30 events/yr in each site. The experiments will take data for about 20 years.

2. The fluorescence detector

The FD comprises 30 telescopes, each one consisting of a large aperture mirror of ~ 3.5 m in diameter, with an array of PMTs in its focal surface, called the FD camera. The aperture of each telescope is $2^\circ-32^\circ$ in elevation and 30° in azimuth. Four hundred and forty hexagonal, 39 mm wide, PMTs at the camera pixelize the aperture in cells of $1.5^\circ \times 1.5^\circ$. To reduce the spherical aberration of the large aperture mirror, a Schmidt optics [5] have been adopted and a diaphragm of 1.7 m is put in front of the mirror at about twice the focal distance (Fig. 1).

Three border "eyes" consisting of a group of six telescopes looking to the center of the site, combined with one central "eye" consisting of 12 telescopes will give fluorescence coverage over almost the whole SD array.

The FD records the trace left at the focal surface by the light spot created by the shower as it develops in the atmosphere. A valid event will trigger a minimum of four to six pixels. The FD signal allows to determine the shower-detector plane (SDP) which contains the detector "eye" and the shower axis. This data together with the SD data on the same event will allow to obtain the best estimate on the energy of the primary, the direction of the shower axis and the primary's composition.

The PMTs have to operate with good linearity independently of the amount of background light that illuminates that pixel. The average background light of dark nights is estimated in 2.7 phel/100 ns although the presence of a single object (a blue star f.i.) in the field of view will increase the photoelectron rate to much higher values.

3. Signal and noise

The FD pixel signal is ideally a trapezoidal current pulse whose rise and fall times are identical and of about $\frac{1}{3}$ the pulse width at the base. The $\sim \frac{1}{3}$ ratio is related to the fact that the light spot progressively enters into the pixel, and its size is

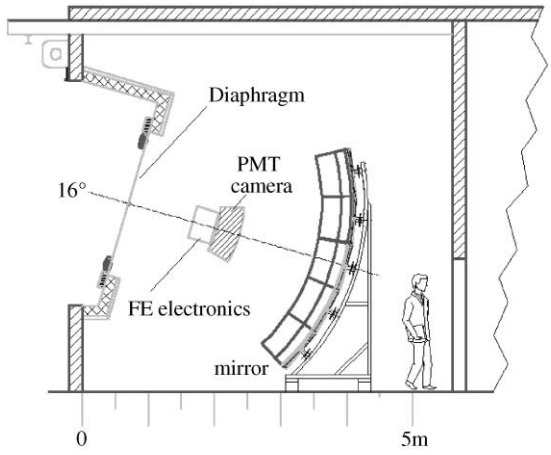

Fig. 1. A fluorescence detector module. The 440 PMTs of the camera are readout by the Head and Front-end Electronics. The total number of channels in each Auger site is 13 200.

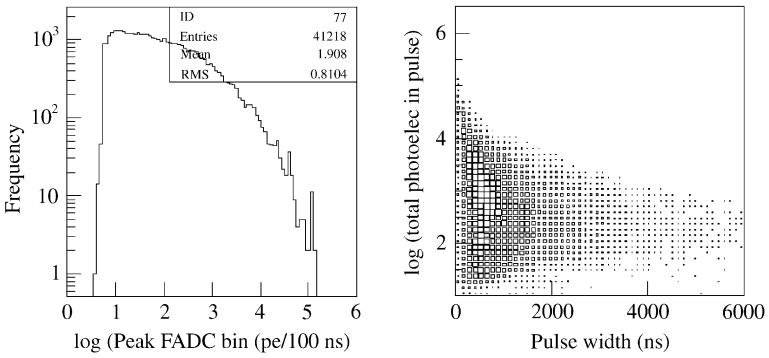

Fig. 2. The amplitude and pulse width at a single pixel for showers of 10^{20} eV [6].

$\sim 0.5^{\circ}$, i.e. $\frac{1}{3}$ the pixel size. Geometrical considerations determine that, at constant energy, both the pulse amplitude and its width are widely variable. The pulse-width, in fact, varies from 100 ns to about 6 μs and the current amplitude from 2 phel/100 ns (3.2 pA) to 131 000 phel/100 ns (210 nA), Fig. 2.

The dynamic range of the current amplitude extends over 16 bit. The noise is mainly determined by fluctuations of the sky-background light. The mean photoelectron rate due to the background is estimated in 2.7 phel/100 ns. It can be noted that for the minimum signal, the total mean photoelectron rate will be 4.7 phel/100 ns or 47 MHz. By filtering the anode signal well below that frequency, a smoothed current pulse is obtained with an amplitude $I_{\mathrm{a}}\ [p\mathrm{A}] = 1.6 \times G \times 2$ phel/100 ns over the mean background current; G is the PMT gain. The noise spectral power density for a signal amplitude I_{sign} above the background is $S_i = 2q(I_{\mathrm{bck}} + I_{\mathrm{sign}})(1 + v_G)G^2$, where v_G ($v_G \sim 0.45$) is the relative variance of the PMT gain [7]. For a PMT gain of 50 K the sky-background current alone has a noise spectral density $i_{\mathrm{n}} = \sqrt{S_i}$ of 71 pA/$\sqrt{\mathrm{Hz}}$. A requirement to the front-end electronics is that the overall noise should not be higher that 10% over the sky noise. This puts a limit to the total noise of the readout chain which has to be therefore $\frac{1}{2}$ the sky noise.

The assumed relatively low gain (50 K) for the PMT assures that its life will be compatible with the expected 20 years of the experiment's running time.

4. System architecture

The readout system was conceived to fulfill the following functionalities:

- readout the FD signal with high linearity and best S/N ratio;
- satisfy the requirements of a 16 bit dynamic range;
- sample the smoothed signal every 100 ns;
- readout the mean sky-background current with very high resolution;
- check the functionality of the overall readout system even with the PMTs HV bias off;
- generate test trigger patterns and
- assure very low failure rate over the experiment's life.

The FD camera consists of 440 eight-dynodes PMTs (Photonis XP3062) arranged in 20 columns of 22 pixels/column. The Front-end Crate, put behind the Camera, allocates 22 Front-end Boards (FEB) each one consisting of the Analog Board (AB) and the Digital Board (DB) which are interconnected together via three high-density 50 pin edge connectors. Each FEB serves all 22 pixels in a column. In this work, we will concentrate on the main blocks of the Analog Signal Processor, which comprises all the hardware elements between the PMTs and the DB of the FEB, i.e. the Head Electronics, the Distribution Board, the Analog Board and the HV and LV power supplies.

A block diagram is given in Fig. 3, a photograph of an HE unit and the AB is given in Fig. 4.

4.1. The head electronics

The Head Electronics (HE) unit consists of two circular PCBs of 32 mm diameter interconnected together by means of three 2-pin connectors. The Bias PCB is soldered to the flying leads of the PMT and interfaces with the DC anode current monitor system. The Current Monitor/Driver PCB contains the PMT anode resistor, AC coupling network, signal driver, DC anode current monitor and test pulse injection network. A first batch of 150 units have been fabricated and fully tested on August 1999. Results of the test show very uniform characteristics. A comprehensive report on the HE unit and on the results of this first test is given separately [8]. We summarize in this section its main features. At the moment of writing this paper, a second batch of 350 units is under fabrication.

4.1.1. Bias network

The HE provides an active bias network which includes three high-voltage bipolar transistors (BITs) to stabilize the potentials of the last three dynodes. Low-cost small-outline surface-mount BJTs, nowadays readily available, were used for this purpose (FMMT458). Compared to a classical passive resistor network, the active network shows a dramatic reduction of power dissipation and a large improve in the PMT linearity even when large DC background current is circulating in the anode. In fact, the active network, dissipating 131 mW, has a 2% gain increase for a DC anode current of 20 μA. A passive network instead dissipates 246 mW and at 20 μA its gain varies by 10% [9]. Reduction of power consumption has a large impact in the cost of the HV power supplies required for the full-size detector.

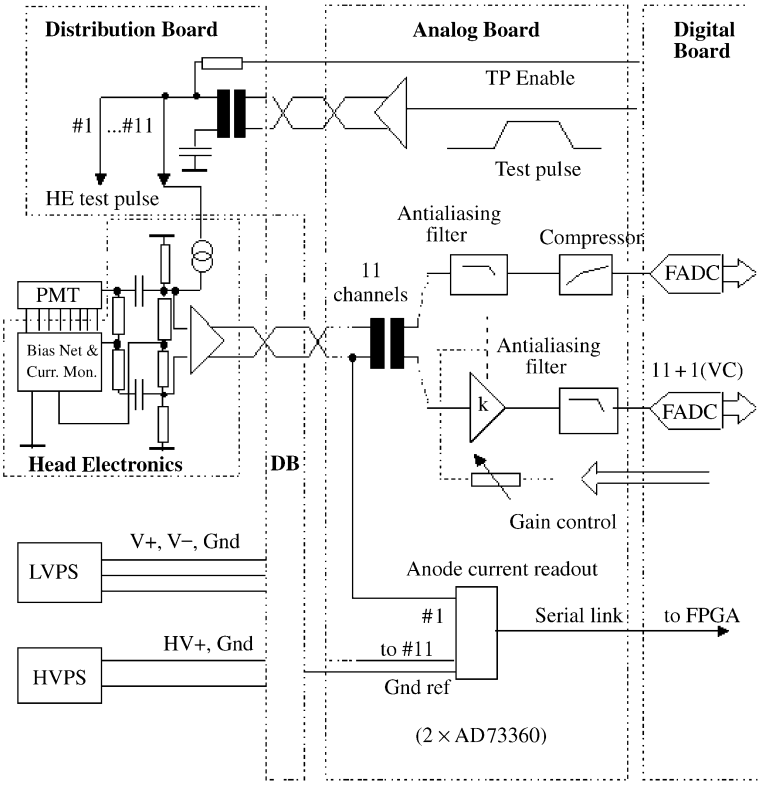

Fig. 3. A block diagram of the FD Analog Signal Processor. The modularity of the system is 11 channels.

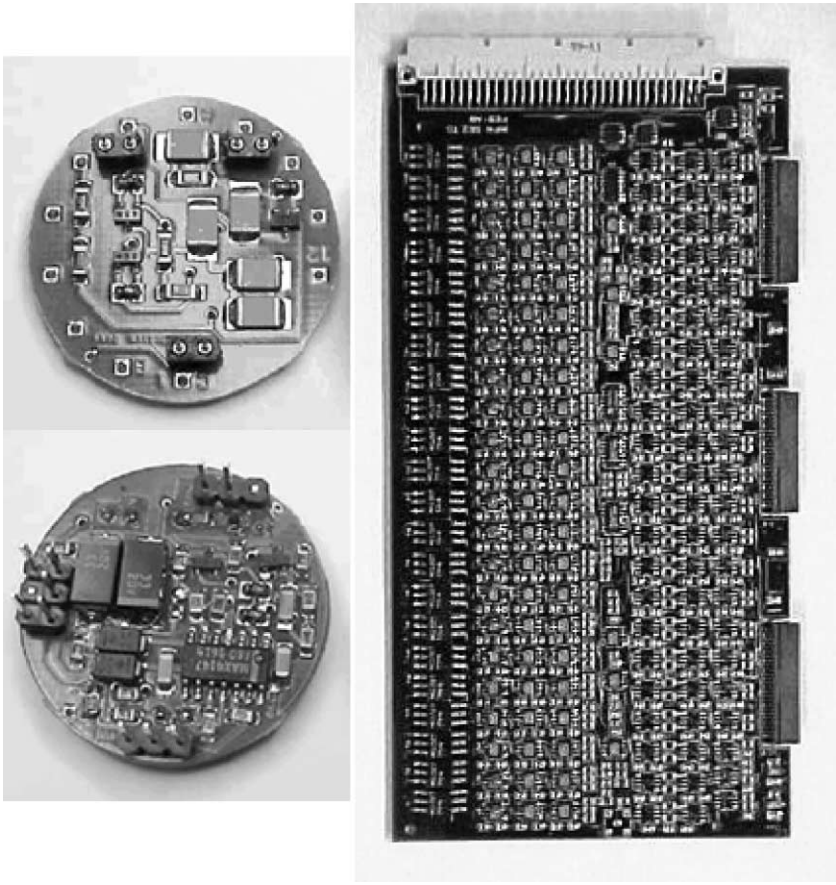

Fig. 4. The Bias and Driver/CM PCBs of the HE unit and the Analog Board (not in scale).

4.1.2. Signal driver

To have a large reduction of common-mode noise, a fully differential configuration was adopted to readout the PMT FD signal. A symmetrical network at the driver's input (a MAXIM 4147 ESD) receives the FD signal only through the leg which is actually connected to the PMTs anode. The second leg is identical to the first one but it is not connected to the PMT (see Fig. 3). It can be shown that the pulse produced at the non-inverting output of the signal driver is negative going and has and amplitude of $\times 1.5$ the input pulse. At the inverting output instead, it is a positive-going pulse with an amplitude of $\times 0.5$ the input pulse. In summary, a pulse with an amplitude a factor $\times 2$ the input pulse travels differentially through twisted pairs to the DB and from there to the FEB. To take best profit of the driver's linear range the driver is DC biased at ~ 1.9 V. This gives the larger, negative going pulse, more room before reaching the saturation region. The rejection to the common mode noise was determined by measuring with a spectrum analyzer the transfer function from the HV input to the FEB input. A common-mode rejection ratio (CMRR) of 28 dB in the range 1–100 kHz was determined [8].

4.1.3. Current monitor

So far the measurement of the DC anode current of a positive biased PMT could be per-formed only indirectly through the measurement of the fluctuations in the baseline. Sensitivity of this method is low as the fluctuations are

proportional to the square root of the current. In addition, external noise sources, not coming from the sky-background light, could introduce additional errors. Measuring with high-resolution the DC anode current in every pixel is desired to evaluate the sky quality and at the very same moment an FD pulse is also recorded. Knowing the sky conditions (atmospheric attenuation, presence of clouds or bright objects and others sources) gives important information for the event reconstruction. For that purpose, a novel method to measure the DC anode current of a grounded cathode PMT has been developed [10]. The system is based on an optically coupled current mirror,[2] whose principle of operation is illustrated in Fig 5.

A combination of a linear optocoupler illuminating two photodiodes and a standard optocoupler followed by a high-current gain stage form a feedback loop in which both the action and the feedback paths are optically coupled. The high-current gain on the action path determines that virtually all the current I to be measured circulates through the first photodiode, and it is therefore replicated at ground level at the second photodiode. A precise, temperature-independent measurement of the DC current circulating through a passive input is performed.

As shown in Fig. 3, the current monitor output is used to set the DC bias at the driver's output. This DC common-mode voltage level is linearly related to the mean anode current. The mean anode current signal travels on the same wires that transmit the FD signal. At the FEB, a six-channel 16-bit sigma-delta converter chip (AD 73360) makes a reading at 1.2 KHz. The first measurements of the sky using this method have been performed using a 13 cm diameter telescope. A result is shown in Fig. 6.

In that figure, the dark sky background is clearly distinguished from the full dark level (telescope cup on). The stars slowly enters the telescope field. The small fluctuation during the trailing edge was due to a faint cloud passing by at that moment.

[2] INFN patent pending.

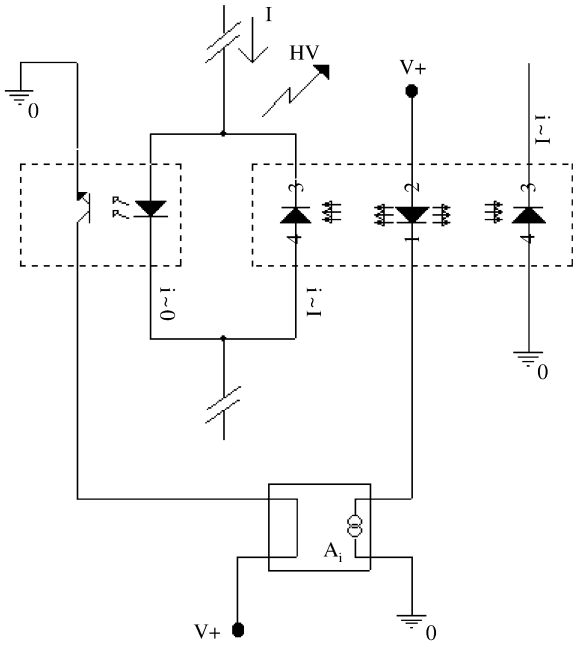

Fig. 5. Principle of operation of the optically coupled current mirror.

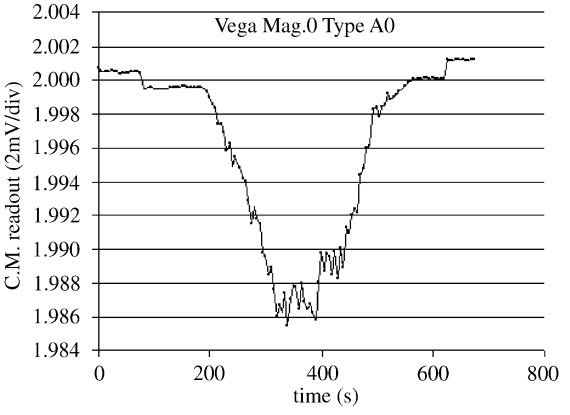

Fig. 6. Response of the current monitor to a blue star: first part of the baseline corresponds to no light in the telescope, then the sky background and finally the star signal.

4.1.4. Test pulse

The HE is provided with a test-pulse input which allows to emulate an FD signal by injecting a current pulse with the desired shape to the very

same node where the PMT does it. This allows operation and testing of the whole readout system even with the PMTs HV bias switched off. The system uses a bipolar transistor connected in common base configuration. A voltage pulse injected through a resistor in series with the emitter is converted into a current pulse. The test signal is delivered by an external, programmable pulse generator connected to the FEB. There, two drivers per AB deliver the test pulse simultaneously to 11 channels in a column. Only one group (upper or lower pixels) are excited at a time. In the next version of the analog board a gating system will be introduced to allow selection of any one pixel to enter at a time. This way the generation of trigger patterns will be possible. The test-pulse system, which is linear over more than three decades, is described in detail separately [11].

4.2. The analog board

The Analog Front-End Board (AB) receives the signal via twisted pair cables from the Head Electronics units after passing through the Distribution Board. The Analog Board processes the signals from 22 PMTs as described in the following and presents them to the FADCs located in the First-Level Trigger Board (FLTB). The following functions must be performed in the AB:

- receiving the signals transmitted by the Head Electronics on the twisted-pair cables, performing a differential-to-single-ended conversion;
- adjusting the gain to compensate for the gain spread of the PMTs;
- adapting the dynamic range of the PMT signals to the input dynamic range of the FADC;
- providing an adequate signal filtering to prevent aliasing;
- reading out the DC level at the twisted pair cables, as it is linearly related to the background illumination at the pixel.

The differential-to-single-ended conversion is done by a transformer. This solution has the advantages, as confirmed by laboratory tests, of adding negligible noise, of providing galvanic decoupling (no ground loops) and of dissipating no power. The time constant introduced by the transformer is $\sim$ 250 μs, so a wide pulse ($\sim$ 10 μs) will have a drop of 4%. The analog channels outputs are connected to 12-bit FADCs sampling the signals at a 10 MHz frequency. According to the criteria discussed in Ref. [12], the bandwidth of the signals presented to the ADC is limited by an antialiasing third-order Bessel filter with a 1.5 MHz cutoff frequency. The filter parameters are chosen to minimize the residual error in the signal amplitude reconstruction from the samples taken by the ADC. Timing requirements may determine a higher cut-off frequency.

4.2.1. Dynamic signal compression

The system was designed to handle a 16-bit dynamic range of signals from the PMTs, therefore, requiring a compression scheme in order to work with a 12-bit FADC. Two solutions are implemented in the prototype phase: the analog compressor and the virtual channel. As described in detail in Ref. [13], the compressor operates on the signals in a non-linear way by means of a bilinear transfer characteristic. Instead, the virtual channel solution exploits the fact that the fluorescence detector signal appears sequentially in neighboring pixels and large amplitude pulse events occupy, at the same 100 ns time slot, only one of 11 non-adjacent channels. The signal from each PMT pixel is processed by a 12-bit linear high-gain channel. At the same time, signals from 11 non-adjacent pixels are added in a low-gain summation (or OR) channel (Virtual Channel) and sent to a FADC. This channel is readout when anyone of the group of the 11 high-gain channels is saturated. Compared to a normal channel, the summation channel features a $\sqrt{11} = 3.3$ times higher noise, but processes large signals only. The Virtual Channel architecture requires two additional channels per board. In both the solutions to dynamic range adapting, a gain control capability is provided to compensate for the gain spread of the PMTs. This is done by adjusting the value of digitally programmable potentiometers in the gain stages. The system is able to accommodate for a factor of 2 variation of the PMT gain above and below the nominal value.

4.2.2. DC anode current readout

As said in Section 4.1.3, the DC voltage at the twisted pair wires entering the analog board is linearly related to the mean anode current in the corresponding pixel. A novel multichannel 16 bit ADC chip (AD 73360) reads out six channels with very high resolution. Four such chips are serially interconnected in cascade through their serial ports and communicates with a FPGA at the digital board where 22 registers keep record of the background light intensity in each pixel. The signal bandwidth is set by a single-pole filter cutting at 9 Hz. This bandwidth is sufficient to allow recording of relatively rapid background fluctuations if desired. The resolution is 0.4 nA of anode current which, for a PMT gain of 50 K, means a 0.2% for the minimum expected background light (2.7 phel/100 ns). The high resolution allows to recognize even faint objects in the pixel's field of view, like tiny clouds, as shown in Fig. 6.

4.2.3. Test pulse drivers

Use of an external pulse generator for the whole mirror allows to emulate fluorescence pulses of different shapes. The pulse generator enters all 22 FEBs in parallel. At each board, two differential drivers of the same type used in the HE units (MAX 4147) distribute the pulse to the two groups of 11 channels in each column.

5. Summary and conclusions

We have designed and constructed an analog signal processing system which incorporates new features compared to previous FD detectors like Fly's Eye [3] and High Res [14]. These features are listed below:

- Active bias network to reduce the HV power consumption by 50%. These bias network keep virtually constant the PMT gain even for large sky background current. At a factor 30 above night sky the gain increases only by 2%.
- Differential signal readout and driving for high common mode rejection ratio.
- Low-noise driver at the HE plus a pulse transformer at the FEB for a 12% increase over dark sky noise.
- Test-pulsing system linear over more than three decades. The system allows to emulate FD signals of virtually any desired shape. An extension incorporating pixel selection will allow to generate trigger patterns. Fault tracing is strongly facilitated.
- Direct measurement of the mean anode current, despite the PMT is biased with positive high voltage (cathode-grounded). Among other possibilities, this novel feature allows to track blue stars to assess the sky quality and to check the stability of the camera alignment.
- Compression of the 16-bit dynamic range into 12 bits. At present two solutions to this problem are under study: the compressor and the virtual channel options.

We are getting ready to arrive to the test of the Auger "Engineering Array" (one FD module plus 40 SD tanks) end 2000–2001 with an analog processing system which shall give an unprecedented performance.

Acknowledgements

We thank Paul Sommers, George Cassiday, Harmut Gemmeke, Matthias Kleifges and Jonny Kleinfeller for the fruitful discussions.

References

[1] J. Linsley, Phys. Rev. Lett. 10 (1963) 146.
[2] M.A. Lawrence et al., J. Phys. G 17 (1991) 773.
[3] D.J. Bird et al., Astrop. J. 424 (1994) 491.
[4] S. Yoshida et al., Astrop. Phys. 3 (1995) 105.
[5] Auger Collaboration, The Pierre Auger Project Design Report, Fermilab, 1995 (http://www.auger.org/admin/).
[6] B. Dawson, GAP-99-038, available at previously cited web site.
[7] Philips Photonics, Photomultiplier Tubes: Principles and Applications, pp. 3–15.
[8] D.V. Camin et al., GAP-99-043, available at previously cited web site.
[9] S. Argirò et al., GAP-99-015, available at previously cited web site.

[10] S. Argirò et al., Nucl. Instr. and Meth. A 435 (1999) 484.
[11] D.V. Camin et al., GAP-2000-029, available at previously cited web site.
[12] P.W. Cattaneo et al., GAP-99-005, available at previously cited web site.
[13] P.F. Manfredi et al., Nucl. Instr. and Meth. A 461 (2001) 526, these Proceedings.
[14] S. Crobato et al., Proceedings of the International Workshop to Study Cosmic Rays with Energies greater than 10^{19}, Paris; Nucl. Phys. B (Proc. Suppl.) 28B (1992) 36.